A close variant of this preprint was published Medical Physics 24:1671-8, 1997.

Three-dimensional reconstruction of curves from pairs of projection views in the presence of error. I. Algorithms

Bullitt E, Liu A, Pizer SM

Division of Neurosurgery, Department of Surgery (EB), Department of Computer Science (AL, SMP), Departments of Biomedical Engineering, Radiology, and Radiation Oncology (SMP)

University of North Carolina, Chapel Hill, NC

Corresponding author:

Elizabeth Bullitt MD

Division of Neurosurgery

CB 7060, 148 Burnett-Womack

University of North Carolina

Chapel Hill, NC 27599

Telephone: (919) 966-1374

Fax: (919) 966-6627

email: bullitt@med.unc.edu

Supported by P01CA47982, R01CA67812 from NCI-NIH.

ABSTRACT

We have previously described an approach to 3D intracerebral vascular reconstruction that uses an MRA as a reconstruction base. Additional vessels seen only by angiography are added by segmenting 2D curves from projection angiograms and reconstructing these curves into 3D, building upon the MRA.

Intracerebral vascular reconstruction is difficult for at least two reasons. First, 2D curves must be associated on projection images even when the human eye cannot do so. Second, 3D curves must be reconstructed in the presence of errors such as misregistration, image distortion, and misdefinition of 2D curves.

This paper is the first of two that address the specific issue of reconstruction of a 3D curve from a given pair of 2D curves in the presence of error. The method explicitly separates what can and cannot be determined from a pair of projection views. It is also capable of recognizing interruptions produced by viewplane errors, of continuing reconstruction beyond such interruptions, and of localizing and estimating the magnitude of the interruptions. These measurements can also be used to estimate the lengths of regional disparities between a pair of 2D curves, leading to a quantitative estimate of the capacity of a pair of 2D curves to combine to create a 3D object *(match value)*. Match values can be used, in turn, as part of the strategy for automatically associating pairs of 2D curves.

This paper provides methods for reconstructing a given pair of 2D curves into 3D in the presence of error and for calculating match values. Error analysis is given in the companion report.

KEY WORDS: angiography, intracerebral vessels, few-view reconstruction, 3D curve, vascular reconstruction

I. INTRODUCTION

For the neurosurgeon, it is often necessary to visualize intracerebral vascular anatomy in three dimensions (3D). Two general types of vascular imaging studies are available. The first type is projection angiography (angiography or angiograms). The second type is direct 3D imaging, as magnetic resonance angiography (MRA) or computed tomographic angiography (CTA). Unfortunately, no single imaging modality provides sufficient information. For example, the 3D imaging techniques often fail to delineate critical vessels[1, 2,3, 4,5]. Clinicians therefore routinely request angiography, which provides more information. Unfortunately, angiograms provide a fixed point of view, are difficult to interpret, and cannot be mapped to 3D datasets[6,7] . It would therefore be advantageous to provide a 3D map of the intracerebral vasculature at an angiographic level of detail.

A detailed, 3D map of the intracerebral vasculature might be produced through 3D reconstruction of angiographic data. Reconstruction of intracerebral angiograms is, however, difficult for several reasons. First, the intracerebral circulation is so overlapped on projection that the human eye cannot associate many points or structures on separated views. Second, angiographic acquisition involves radiation exposure and the injection of toxic contrast material, thus limiting the number of views available. Finally, there are many sources of error, including misregistration, mistakes in definition of 2D curves, projection overlap, and image distortion. Despite attempts by many excellent groups, intracerebral vascular reconstruction is a problem that has defied a clinically useful solution.

We have previously proposed an approach to 3D angiographic reconstruction that employs 2-3 angiographic views and an MRA obtained from the same patient[8] . The MRA is used as a 3D reconstruction base. Angiographic information NOT included in the MRA is incorporated by progressively adding new vessels reconstructed from pairs of 2D curves segmented from the angiograms. Specific steps include segmentation of the image data by core-based methods[9,10] and registration of each angiogram with the MRA[11]. We have used these methods to reconstruct aneurysms seen by angiography into 3D, inserting them into the MRA[12].

For more complex reconstructions, it is necessary to reconstruct 2D curves into 3D in the presence of error. One must also select which 2D curve, curve portion, or set of curves on view B is associated with each 2D curve on view A. We have previously described a method of automatically associating 2D curves which depends upon an estimate of the capacity of a pair of 2D curves to combine to produce a 3D object (the *match value* of a given 2D curve pair)[13]. This match value is, in turn, calculated automatically by a method of reconstructing a given pair of 2D curves into 3D. This 3D curve reconstruction method is also capable of recognizing interruptions produced by viewplane errors, of continuing reconstruction beyond such interruptions, and of localizing and estimating the magnitude of the interruptions.

This paper is the first of two that focus upon the specific problem of reconstructing a given pair of 2D curves into 3D in the presence of error. The current report discusses the method of 3D curve reconstruction and of match value calculation. The companion report provides error analysis [14]. Methods of automatically associating 2D curves on intracerebral angiograms and tests of these methods in simulated angiographic data are given elsewhere[13], but depend upon the curve creation methods described here.

II. THEORY

A. Overview and definitions

A tubular object, both in 2- and 3D, can be defined as an object possessing a central skeleton with an associated width (in 2D) or diameter (in 3D) at each skeleton point. For a 3D tube, the projection of the object's skeleton generally coincides closely with the skeleton of the object's projection. In theory, one can therefore recreate a 3D skeleton curve by reconstructing into 3D the 2D skeletons of a pair of the 3D tube's projections. The diameter of the reconstructed tube is calculated by the viewing geometry, the location of reconstructed points, and the widths of the 2D tubes. We use the terms *2D curve* and *3D curve* to refer to the skeletons of 2- and 3D tubular objects. This paper discusses methods of pairing points along pairs of 2D curves to create 3D curves.

When dealing with complex projection images such as intracerebral angiograms, there may be no simple one-to-one mapping between the curves defined from view A and the curves defined from view B. Angiograms contain overlapping projections. Continuous, complete delineation of a vessel projection as a single 2D curve is therefore often impossible. Although we reduce the problem by using an MRA to define the region of heaviest projection overlap, methods of 3D curve creation must still deal with 2D curves missing an initial sequence of points and with long vessel projections broken by crossing projections into a chain of short 2D curves.

Reconstruction of a pair of angiographic views also requires association of 2D curves. Our method of automatic curve association employs 2D connectivity information, 3D connectivity constraints, and a means of evaluating the quality of match of any given curve on viewA with any given curve on viewB[13] . The purpose of the current paper is to describe our method of 3D curve reconstruction, which is both capable of operating in the presence of error and of providing a quantitative estimate of the quality of match of any given pair of 2D curves.

For reconstruction of a given pair of 2D curves, we, like many groups, employ the rules of epipolar geometry. Assume 2 perfectly registered point ray sources and two viewplanes. The *epipolar plane* associated with a 3D point is defined by that point and the 2 ray sources. The same plane is also defined by the 3D point and its 2 projections. An epipolar plane intersects a viewplane along an *epipolar line*. For each 2D projection point, the epipolar line restricts the search for the paired point on the second view to a one-dimensional neighborhood[15, 16, 17].

Reconstruction from angiograms must deal with several sources of error. We define *viewplane error* as any error in the set of points defining a 2D curve. This paper describes a general means of 3D curve reconstruction in the presence of error, regardless of cause.

B. Reconstruction of a point from a pair of viewplane pixels

Consider a point in 3D space that is projected without error upon two viewplanes. Each projection point represents a ray between a ray source and the 2D point. If a 3D point is reconstructed by intersecting these two rays, the original point is recreated exactly.

The case is different when 2D curves are defined in pixels. Each pixel represents the 2D area within which a 3D point may project. The situation can be modeled by viewing each pixel as a pyramidal ray with a tip at the ray source. A ray intersection then becomes a pyramid-pyramid intersection. A volume of uncertainty surrounds each reconstructed point. The term *pixel intersection* refers to an intersection between the spatial pyramids defined by a pixel pair.

C. Inherent limitations of 3D curve reconstruction from a pair of 2D curves

A problem inherent to 3D reconstruction from an image pair is that multiple 3D curves can project identically upon two viewplanes. Consider two viewplanes and an arbitrary epipolar plane. Now imagine some figure lying in this plane. No matter what the figure's shape, it will project as a straight line upon each viewplane (Fig 1). It is impossible to reconstruct the course of a 3D curve while consecutive strings of 2D points lie within the same epipolar plane on both views.

When pixels are used for reconstruction, the epipolar plane becomes a volume. We term this generalization of the epipolar plane the *epipolar volume*. Similarly, each pixel becomes associated not with an epipolar line but with an *epipolar region*. Under perspective projection, the epipolar volume resembles a box with 3 crushed corners (Fig. 2). The course of a 3D curve is indeterminable within this volume. In other words, when a string of consecutive 2D points courses within an epipolar region, only the first point entering and/or the last point leaving the region provide useful information.

D. Reconstruction in the presence of viewplane errors

Viewplane errors can displace point projections on the viewplane. If projection points are infinitely small, the ray associated with each 2D point is infinitely thin. Even a minuscule error in the placement of a projection point may prevent intersection of a pair of associated rays. The 3D point defined by these rays then cannot be reconstructed. Reconstruction will stop.

One way of handling this problem is to view each viewplane "point" as fuzzy. Defining 2D curves in pixel units (and thereby each ray as a pyramidal volume) creates fuzzy 2D points. Viewplane errors that displace a 3D point projection within the same pixel as the true point projection will not interfere with reconstruction since the pyramidal rays defined by each pixel will still intersect correctly. The larger the pixel, the greater the protection against viewplane error. However, the larger the pixel, the greater the uncertainty of the placement of each 3D point. The companion paper discusses the topic of pixel size in more detail[14].

We term a viewplane error that results in displacement of a 2D projection point within its correct pixel as a *minor viewplane error*. Minor viewplane errors do not affect reconstruction accuracy. *Major viewplane errors* include a missing sequence of points at the start of one 2D curve or displacement of a projection point outside of its correct pixel. Major viewplane errors often preclude intersection of a pair of associated rays, bringing reconstruction to a stop.

We do not have methods that can guarantee accurate reconstruction in the presence of major viewplane errors. However, as outlined below, we do have methods to detect and continue reconstruction beyond interruptions produced by such errors. These methods minimize informational loss, report the length of regional disparities between a pair of 2D curves, and can be used to estimate the capacity of a 2D curve pair to combine to produce a 3D object.

III. METHODS

A. Algorithms for reconstruction of a 3D curve from a pair of 2D curves defined in pixels

Each 2D curve is a directed curve, with one end known as the start. We do not assume that the start or endpoints of the two 2D curves correspond. Viewplane errors may be present.

The approach is to jump along each 2D curve, using the last defined 3D point and the pair of pixels that created this point to determine an epipolar volume. The course of the 3D vessel is indeterminate within this volume. However, once the 3D object's path courses beyond this volume, the next appropriate pixel pair can be identified along each 2D curve. This pixel pair creates a new 3D point and a new epipolar volume. Subroutines described later are given in bold face. Major viewplane errors are handled by a directed search, as discussed later.

The general algorithm is as follows:

1. Do a **directed search** for a first 3D point
2. If the search was successful output the 3D startpoint; otherwise return
3. While points remain along both 2D curves {
4. Find and jump to the **next appropriate pixel** along each 2D curve
5. Test the pixel pair for a pixel intersection

6. If the expected pixel intersection is not present {

7. Perform a **directed search** to find a pixel intersection

8. If no intersection is found break from the loop

9. }

10. Output the new 3D point

11. } //end while loop

The program first searches for a startpoint along each 2D curve (1). If a startpoint is found, the program enters a loop (3-11) to produce consecutive 3D points. Major viewplane errors are handled (6-9) by conducting a directed search for a nearby solution, as discussed below.

1. Jump to the next appropriate pixel along a 2D curve (line 4)

Given a 3D point and the two pixels used to create it, it is necessary to search forward along each 2D curve for the first pixel outside of the current epipolar volume. A rapid means of selecting the desired pixel is to test each consecutive pixel for an intersection with the pixel on the opposite view used to create the last 3D point. On each 2D curve, the first pixel that fails the intersection test is the first pixel outside of the current epipolar volume. In the absence of error, this pixel pair produces an intersection, a new epipolar volume, and smooth continuation of reconstruction.

The number of pixels skipped along each 2D curve is neither uniform during each function iteration nor the same on each view. On average, for viewplanes subdivided into 1024x1024 pixel units, one out of every 2-3 pixels along a 2D curve is used to create a 3D point.

2. Performing a directed search along a pair of 2D curves (lines 1 and 8)

A directed search along paired 2D curves is necessary when the start of one curve is missing points or when two pixels do not produce an expected intersection. In such cases, the program considers itself “lost” and attempts to recover by searching for a nearby pixel along each 2D curve such that this pixel pair produces an intersection. Searches terminate successfully when a pixel intersection is found, allowing reconstruction to continue. Searches terminate unsuccessfully when a 2D curve runs out of points. Searches terminate unsuccessfully with a warning that there is a serious discrepency between the pair of 2D curves when the search exceeds a predefined maximum distance or when a ray pair examined during the search is separated by a predetermined maximum distance.

Designing effective search algorithms is difficult because a looping 2D curve may cross the same epipolar region many times. There are often several ways to pair 2D curve segments. Different search methods produce different solutions. A poor search method uses epipolar lines to find the first pixel on view B that intersects the pixel on view A when two selected pixels fail to intersect. Figure 3 illustrates the disadvantage of this approach. A better solution is to select pixels along each 2D curve close to the pixel pair at which the program first became lost. A nearby solution will “hold” the two 2D curves together, preserving maximum information.

Assume that a pair of pixels does not produce an expected intersection. The program is now lost and initiates a search. Call the 2 pixels “lostA” on view A and “lostB” on view B. The term “lostA +1” indicates the next pixel after lostA along the 2D curve on view A. The search queries pixels along curves A and B in the order (lostA +1, lostB), (lostA, lostB + 1), (lostA +1, lostB +1), (lostA +2, lostB), etc. The first pixel pair to produce an intersection is selected, and the program continues. A count is kept of the number of pixels skipped by the search.

This kind of directed search provides a number of pieces of useful information about regional discrepancies between a pair of 2D curves. First, a search is initiated only when the start of one 2D curve is missing points or when, during reconstruction, a selected pixel pair fails to make an expected intersection. The initiation of a search is therefore an automatic indication of error.

Second, successful completion of a search results in a jump along one or both 2D curves. The number of pixels jumped provides an estimate of the magnitude of error. For example, with viewplanes of 1024x1024 pixels, a search jump of 1-2 pixels is of little consequence but a jump of 25 pixels may indicate a 5 mm gap in the reconstructed curve.

Finally, each search is bounded both in 2- and 3D. Since the program is automatically aware where each error occurred, a 3rd view could be used to fill in missing data.

B. Match value calculations

The above techniques can be used to estimate the capacity of a 2D curve pair to combine to produce a 3D object. We term this estimate the *match value* of the 2D curve pair.

Most intracranial vessels change direction frequently. In the absence of error, a pair of 2D curves representing projections of the same 3D object produce a smooth reconstruction. By contrast, mismatched 2D curves almost always diverge from each other, producing a reconstruction in which the program becomes “lost”.

Calculating the match value of a 2D curve pair begins by taking the number of 3D points produced by reconstruction of the 2 curves. A pair of curves that never intersect each other have a match value of 0 (Fig 4a). A pair of curves that combine perfectly with each other have a match value equal to the number of points produced by reconstruction of the pair of 2D curves (Fig. 4b).

It is common for a pair of 2D curves to combine to provide a sequence of 3D points but for the curves to have regions of divergence, resulting in a directed search. A penalty is imposed for directed searches proportional to the length of the search. At present we define this penalty by the simple formula, based upon results in our test data, of 1 point for each 6 consecutive pixels jumped. The match value is decreased by this amount, thus reducing the value of a reconstruction in which a 2D curve possesses strings of points that do not correspond to the second curve (Fig. 4c-d). Sometimes a directed search terminates because the 2D search range is exceeded or because two rays examined during the search are widely separated even at their closest point. In these cases the 2D curves diverge from each other too much to provide a good match. The match value for this pair is set to 0 (Fig. 4e).

The above examples apply when a pair of 2D curves represent approximately the same segment of a 3D curve. Projection overlap will often interrupt a vessel projection, however, producing a sequence of short 2D curves separated by crossing projections. We call a sequence of 2D curves, interrupted only by crossing vessels, a *curve chain*. What happens when a long curve on one view maps to a curve chain on the other?

Suppose curveA maps to a curve chain whose first curve is curveB1. The match value of curveA-curveB1 will then be calculated differently than the match value of curveB1-curveA. The final match value of curveA-curveB1 is determined as the sum of match values produced by sequential mapping of curveA with each curve in the chain (Fig. 4f). If more than one possible curve chain originates from curveB1, the program will automatically calculate all possibilities and assign the maximum total match value to the curveA-curveB1 match. The match value of curveB1-curveA, however, is only the match value produced by reconstruction of the short curveB1 with a portion of the longer curveA. This method makes it possible to compare the match values of curveA with any curve on view B (and vice versa) regardless of curve length.

As discussed by Bullitt[13], match values can be used to help associate 2D curves. Each curve on view A has a match value with each curve on view B, and vice versa. Ranking each curve's choices by match value helps estimate the likelihood that a pair of curving, looping, 2D curves are associated. If the match value of both curveA-curveB and of curveB-curveA are high relative to alternative choices, the two curves are very likely to be associated.

C. Tests of reconstructing a pair of 2D curves into a 3D curve

We used simulated angiographic data to test the method of reconstructing a given pair of 2D curves into a 3D curve. Sets of vessels were extracted from an MRA by core-based methods[10] and projected so as to create pseudo-angiographic images. Associated pairs of 2D curves were then reconstructed back into 3D. In this test situation, the "start" end of each 2D curve was automatically known to the program. The widths of reconstructed vessels were calculated from the viewing geometry, the widths of the projections, and the location of each 3D point.

Reconstruction accuracy was evaluated by comparing the 3D coordinates of the reconstructed data to the 3D coordinates of the vessels originally extracted from the MRA. The purpose of this experiment was to evaluate our ability to reconstruct complex, looping 3D curves; the companion paper extends these tests to situations in which progressively severe registration error is present[14]. Tests of automatic 2D curve association were not performed in either report, but are described elsewhere[13].

For testing purposes, we modeled the viewing geometry to simulate clinically used angiographic views. The volume of interest (the patient's head) was positioned by registering an MRA dataset with an antero-posterior (AP) and lateral angiographic view obtained from the same patient, using core-based registration[11]. The source to viewplane distance (91.4 cm) and viewplane size (29.2 cm) mimicked the settings used during angiography. Each viewplane was subdivided into 1024 x 1024 pixels of 0.0285 x 0.0285 cm. The magnification factor was approximately 1.8.

2D curves were artificially created by projecting each vessel skeleton upon the 2 viewplanes. Each projected point was rounded to its nearest pixel value and non-continuous point projections were connected by linear interpolation, thus providing errors of 2D curve definition. The width of the tubular object associated with each 2D curve was calculated according to the rules of perspective geometry and the width of the 3D vessel used to create the projection.

Reconstruction was performed for 3 different sets of extracted vessels, obtained from two different patients. Each test involved reconstruction of between 40-60 vessels and the reconstruction and analysis of between 1100-1500 reconstructed points. Figure 5 demonstrates, in small windows, the two projection views used for reconstruction of one of these datasets.

D. Clinical accuracy requirements

3D angiographic reconstructions will be used for 2 purposes. The first is to provide a display that clarifies complex vascular relationships for surgical guidance. The second is calculation of 3D coordinates. These two purposes have different accuracy requirements.

Reconstructions for surgical visualization need only be qualitatively accurate. Occasional errors can be tolerated as long as the reconstruction provides useful information about vascular relationships. We judge our test reconstructions as meeting the criteria of clinical utility if

1. The magnitude of mean point displacement is less than 0.2 cm, and

2. A reconstruction appears correct or very close to correct on 3 mutually orthogonal projections when compared to similar projections of the true 3D vessels.

More precision is required for stereotactic surgery, which may not tolerate even a single badly placed point or missing branch. For such procedures, it is important for the surgeon to have some estimate of the maximum gap or maximum point placement error likely to be produced by the program. The tips of stereotactic instruments are generally in the range of 0.1 - 0.5 cm. We therefore add two additional requirements for procedures requiring 3D coordinate information:

3. Gaps in the reconstruction of no more than 0.5 cm, and

4. 3D point placement errors of no more than 0.5 cm.

IV. RESULTS

For all 3 tests, the mean and standard deviation of the distance between reconstructed points and the closest point on the associated true 3D curve was 0.01 $\pm$ 0.01 cm. Each 2D curve mapped from its start pixel to within a few pixels of its end.

The program often became "lost" because of errors in 2D curve definition. In such cases the program announced that an error had occurred, performed a directed search, and then recovered, reporting the number of pixels (generally 1 or 2) that had to be skipped, the length of the gap in the reconstructed vessel, and the 2- and 3D coordinates of the gap. On average, the program became lost once for every 7 3D points plotted, with a mean of 1.8 pixels skipped during each directed search. In one instance a 12 pixel jump occurred, producing a gap of approximately 1.5 mm. No significant point placement errors were produced. All loops were successfully reconstructed into 3D. All reconstructions met all criteria for clinical utility.

V. DISCUSSION

A. Other approaches to 3D curve reconstruction

There is a large volume of literature on the subject of 3D vascular reconstruction[15,18,19, 20, 21, 22, 23, 24, 25, 26, 27, 28, 29, 30, 31, 32, 33, 34]. One means of reconstructing pairs of 2D curves is to manually identify paired points on a pair of projection views[18, 19, 20, 21, 22]. This method has been used successfully to reconstruct the coronary circulation but, for the intracerebral circulation, is too laborious and difficult to be useful.

Fencil and Metz demonstrated elegantly that the relative geometry of two biplane views of unknown orientation can be calculated by the relative positions of 8 object points, and that the exact coordinates of multiple point objects can then be derived[23]. A later paper by the same group showed that this relative geometry can be determined by as few as 5 points, and the authors successfully reconstructed a computer-simulated coronary arterial tree[24]. Their method of registration and reconstruction assumes, however, that one knows the paired projection coordinates of each 3D point.

The use of narrowly separated views makes it easier to associate paired points on complex images. Several groups have therefore investigated 3D intracerebral vascular reconstruction from a pair of narrowly separated views[15, 20, 21, 25, 26, 27]. Creating accurate 3D curves from narrowly separated views is difficult in the presence of error, however[14].

Several investigators have described automatic reconstruction of lines or curves from a sequence of multiple, narrowly separated views[28, 29, 30]. Most angiography units allow acquisition of only 1-2 views at a time, however. The additional time and risk required to obtain a large number of images therefore usually restricts the number of views available.

The Suetens group provided an automated, clinically useful means of reconstruction of coronary vessels, based both upon epipolar geometry and a knowledge-based system specific to the coronary vasculature[15, 25, 31]. Our methods build upon the techniques of 3D curve creation described by this group, adding error handling, quantitative estimation of the capacity of a 2D curve pair to produce a 3D curve, and separation of what can and cannot be known from a pair of projection views.

Another approach to intracerebral vascular reconstruction was recently attempted by COVIRA. This method, like our own, proposed reconstructing additional angiographic data upon an MRA base. The method of 3D curve creation, however, involved rotation of synthetic cylinders whose projections could be compared to curves on projection views[32, 33]. This method appears difficult, especially in the presence of viewplane error, since one does not know in advance either the orientation or the length of each cylinder.

Henri is developing a method that, like ours, uses 2D connectivity information[27, 34]. Henri's method of reconstructing curves, however, uses a pair of projection views to create all 3D points possible by the rules of epipolar geometry. These points are then sorted and ordered to create all possible vessels, producing an "Intermediate Reconstruction" (IR). A 3rd view and principles of connectivity are then used to cull spurious creations. Our match value calculations are in some ways similar to a quantitative, directly calculated IR, in which the continuity of each 2D curve is always preserved and in which information about regional discrepancies between pairs of 2D curves is also obtained.

B. Advantages and disadvantages of our curve creation methods

This report describes a method of reconstructing a 3D curve from a pair of directed 2D curves in the presence of error. Unlike previous approaches, this method can continue reconstruction from a given pair of 2D curves in the presence of viewplane error while simultaneously localizing and estimating the magnitude of errors encountered during reconstruction.

Unlike many approaches, our methods explicitly extract only what can be known from a pair of projection views. The path of a 3D curve is indeterminable within an epipolar volume. We therefore make no attempt to define curves in these areas and so do not have the problem of sometimes creating a plane of points[27]. Instead, the program automatically jumps to the next pixel pair capable of producing meaningful 3D information.

This method produces an ordered but discontinuous set of 3D points. A disadvantage of the method is that gaps may exist in the reconstruction. The fact that the program can bound these gaps both in 2- and 3D, however, means that a third view can be used to fill in missing information. If a third view is not available, the 3D points can be connected by interpolation, providing the best approximation from the information available.

This reconstruction method also automatically assesses the magnitude of interruptions produced by viewplane error or by regional disparities in a pair of 2D curves. Such information, in combination with the number of 3D points produced, provides an estimate of the capacity of a given 2D curve pair to produce a 3D object. This estimate, in combination with 2D connectivity information, provides means of automatic 2D curve pairing[13].

A disadvantage of the current implementation is that reconstruction only moves forward along a directed pair of 2D curves. This means that if a vascular loop appears as a "U" on one view and is seen on edge as a straight line on the second view, only one side of the "U" is reconstructed directly. When such loops are short, the program jumps the gap with little loss of information. For the majority of the circulation and for the majority of clinically used views, such loops are indeed short. However, we know that there are a few areas (e.g., the distal anterior circulation as seen from a straight AP view) that we cannot reconstruct effectively. We now therefore use oblique rather than straight AP views[13]. It would be preferable if the program had the capacity to "back up" under appropriate circumstances. Addition of this ability is one of our goals.

The method described also depends upon directed 2D curves. In the test situation employed here, the "start" end of each 2D cuve was automatically defined. Our segmentation methods also produce directed curves[9]. 3D reconstruction of a pair of directed 2D curves, each with the correct "start" end is fully automatic. If 2D curves are defined by different means, the reconstruction program must be informed which end of each 2D curve is the "start". For reconstruction of a connected vascular tree, the "start" end of each 2D curve could be automatically defined as the end attached to the parent vessel. If reconstruction of disconnected objects is desired, however, the program must be informed manually or by some other means which end of each curve is the "start".

The 3D curve creation paradigm runs reasonably rapidly. Creating and drawing 46 vessels containing 1400 reconstructed points takes 6 minutes on a 66 MHz Pentium computer.

VI. CONCLUSIONS

3D reconstruction of intracerebral vessels is a complex problem whose solution requires accurate segmentation and registration, methods of associating 2D curves, and means of dealing with a variety of potential errors. The current report analyzes the specific problem of reconstruction of a 3D curve from a given pair of directed 2D curves. Advantages of the approach include the abilities to create complex 3D curves in the presence of error, to detect and localize reconstruction errors, and to estimate the capacity of a 2D curve pair to combine to create a 3D object.

ACKNOWLEDGEMENTS

We are grateful to Stephen Aylward for his core-based segmentation and to Dr. Julian Rosenman for use of his computing facilities. Supported by P01CA47982 and R01CA67812 NCI-NIH.

REFERENCES

1. G. Marchal, H. Bosmans, L. Van Fraeyenhoven, G. Wilms, P. Van Hecke, C. Plets, and A.L. Baert, " Intracranial vascular lesions: optimization and clinical evaluation of three-dimensional time-of-flight MR angiography," Radiology **175**:443-448 (1990).

2. S. Napel, M.P. Marks, G.D. Rubin, M.D. Dak, C.H. McDonnell, S.M. Song, D.R. Enzmann, and R.B. Jeffrey, "CT angiography with spiral CT and maximum intensity projection," Radiology **185**:607-610 (1992).

3. W.Y. Guo, B. Nordell, B. Karlsson, M. Soderman, M. Lindqvist, K. Ericson, A. Franck, I. Lax, and C. Lindquist, "Target delineation in radiosurgery for cerebral arteriovenous malformations. Assessment of the value of stereotaxic MR imaging and MR angiography," Acta Radiologica **34**:457-463 (1993).

4. D. Petereit, M. Mehta, P. Turski, A. Levin, C. Strother, C. Mistretta, R. Mackie, M. Gehring, S. Kubsad, and T. Kinsella, "Treatment of arteriovenous malformations with stereotactic neurosurgery employing both magnetic resonance angiography and standard angiography as a database," Int. J. Rad. Onc. Biol. Phys. 25:309-313 (1993).

5. B.E. Pollock, J.C. Flickinger, D. Kondziolka, and L.D. Lunsford, "Indications and expectations of AVM radiosurgery," Contemp. Neurosurg. **18 (6)** :1-5 (1996).

6. D.R. Blatt, W.A. Friedman, and F.J. Bova, "Modifications based on computed tomographic imaging in planning the radiosurgical treatment of arteriovenous malformations," Neurosurgery **33**:588-596 (1993).

7. F.J. Bova, and W.A. Friedman, "Stereotactic angiography: an inadequate database for radiosurgery," Int. J. Rad. Oncol. Biol. Phys. **20**:891-895 (1991).

[8] E. Bullitt, M. Soltys, J. Chen, J.R. Rosenman, and S.M. Pizer, "Three-dimensional reconstruction of intracranial vessels from biplane projection views, " J. Neurosci. Meth. 66,13-22 (1996).

[9] D.S Fritsch, D. Eberly, S.M. Pizer, and M.J. McAuliffe, "Stimulated cores and their applications in medical imaging," in *IPMI '95: Information Processing in Medical Imaging* edited by Y. Bizais, C. Barillot, R. DiPaola (Dordrecht: Kluwer Series Computational Imaging and Vision 1995) pp. 365-368.

[10] S. Aylward, S.M. Pizer, E. Bullitt, and D. Eberly, "Intensity ridge and widths for 3D object segmentation and description," I.E.E.E. W.M.M.B.I.A. 96TB100056, 131-138 (1996).

[11] A. Liu, E. Bullitt, and S.M. Pizer, "3D/2D registration using tubular anatomical structures as a basis," TR # 96-053; Department of Computer Science, University of North Carolina-Chapel Hill, Chapel Hill, NC, 27599, 1996.

[12] E. Bullitt, A. Liu, S. Aylward, M. Soltys, J. Rosenman, and S.M. Pizer, "Methods of displaying intracerebral vascular anatomy," Amer. J. Neuroradiol. 18:417-420, 1997.

[13] E. Bullitt, A. Liu, S. Aylward, and S.M. Pizer, "Reconstruction of the intracerebral vasculature from MRA and a pair of projection views," accepted IPMI 1997, to be published in Lecture Notes in Computer Science (1997).

[14] E. Bullitt, A. Liu, and S.M. Pizer, "Three dimensional reconstruction of curves from projection views in the presence of error. II. Analysis of error," TR # 96-048; Department of Computer Science, University of North Carolina-Chapel Hill, Chapel Hill, NC, 27599, 1996.

[15] C. Smets, "*A Knowledge- Based System for the Automatic Interpretation of Blood Vessels on Angiograms*," Ph.D thesis. (Leuven University Press, Belgium, 1990).

[16] R. Horaud R, and T. Skordas, "Stereo correspondence through feature grouping and maximal cliques," IEEE Trans. Pattern Anal. Machine Intell. **11**:1168-1180 (1989).

[17] D. Vandermeulen, P. Suetens, J. Gybels, and A. Oosterlinck A, "A new software package for the microcomputer based BRW stereotactic system: integrated stereoscopic views of CT data and angiograms," Proc. S.P.I.E. **593**, Medical Image Processing, 103-115 (1986).

[18] N. Guggenheim, F. Chappuis, C. Suilen, P.A. Doriot, P.A. Dorsaz, P. Descouts, and W. Rutishauser, "3D-reconstruction of coronary arteries in view of flow measurement," Int. J. Cardiac Imaging **8**:265-272 (1992).

[19] D.L. Parker, D.L. Pope, K.S. White, L.R. Tarbox, and H.W. Marshall, "Three-dimensional reconstruction of vascular beds," I.P.M.I. **(**Boston:Nijhoff Publishers, 1986) pp. 414-430.

[20] J.M. Rubin, and R.E. Sayre, "A computer-aided technique for overlaying cerebral angiograms onto computed tomograms," Investigat. Radiol. 13:362-367 (1978).

[21] J. Vignaud, P. Rabischong, J.P. Yver, P. Pardo, and C. Thurel, "Multidirectional reconstruction of angiograms by stereogrammetry and computer. Application to computed tomography," Neuroradiol. **18**:1-7 (1979).

[22] A. Wahle, E. Wellnhofer, I. Mugaragu, H.U. Sauer, H. Oswald, and E. Fleck, "Assessment of diffuse coronary artery disease by quantitative analysis of coronary morphology based upon 3-D construction from biplane angiograms," I.E.E.E. T.M.I. **14**:230-241 (1995).

[23] L.E. Fencil, and C.E. Metz, "Propagation and reduction of error in three-dimensional structure determined from biplane views of unknown orientation," Med. Phys. **17**:951-960 (1990).

[24] S-Y J. Chen, and C.E. Metz, "Improved determination of biplane imaging geometry from two projection images and its application to three-dimensional reconstruction of coronary arterial trees," Med. Phys. **24**:633-654 (1997).

25. D. Delaere, C. Smets, P. Suetens, G. Marchal, and F. Van de Werf, "Knowledge-based system for the three-dimensional reconstruction of blood vessels from two angiographic projections," Med. Biol. Eng. Comput. **29**:NS27-NS36 (1991).

26. C.J. Henri, D.L. Collins, and T.M. Peters, "Multimodality image integration for stereotactic surgical planning," Med. Phys. **18**:167-177 (1990).

27. C.J. Henri, and T.M. Peters, "Three dimensional reconstruction of vascular trees: Experimental evaluation," Med. Phys. **23:**617-627 (1996).

28. C. Zhao, and R. Mohr, "New methods of 3D curved object modeling from image contour surfaces," Proc. SPIE Intelligent Robots and Computer Vision XIV: Algorithms, Techniques, Active Vision, and Materials Handling **2588**:348-359 (1996).

29. Y-L Chang, and J.K. Aggarwal, (1995) "Representing and estimating 3D lines," Pattern Recognition **28**:1181-1198 (1995).

30, T. Papadopoulo, and O. Faugeras, "Computing structure and motion of general 3D curves from monocular sequences of perspective images," Computer Vision E.C.C.U. 1996 4th European Conference on Computer Proceedings **2**: 696-708 (1996).

31. C. Smets, G. Verbeek, P. Suetens, and A. Oosterlinck, (1988) "A knowledge-based system for the three dimensional reconstruction of the cerebral blood vessels from a pair of stereoscopic angiograms," in *Pattern Recognition and Artificial Intelligence,* edited by E.S. Gelsema, and L.N. Kanel, (Elsevier, North Holland, 1988) pp 425-435.

32. M. Bahner, J. Dick, B. Kardatzki, H. Ruder, S. Matthias, A. Steitz, C. Bertram, D. Hentschel, T. Hidebrand, E. Hundt, R. Kutka, S. Stier, G. Gerig, T. Koller, O. Kubler, and G. Szekely, "Combining two imaging modalities for neuroradiological diagnosis: 3D representation of

cerebral blood vessels," in *Data Fusion Applications* edited by Pfleger (Research Esprits Esprit, Project 5354 DIMUS, Vol 1, Springer-Verlag, Heidelberg, 1993) pp. 1 - 16.

33. M. Bahner, J. Dick, B. Kardatzki, H. Ruder, M. Schmidt, and A. Steitz, "Reconstruction of the 3D structure of cerebral vessels from few DSA` projections," in *Computer Assisted Radiology: Proceedings of the Intrnational Symposium Car*, edited by H.U. Lemke, K. Inamura, C.C. Jaffe, and R. Felix (Springer-Verlag, Heidelberg, 1993) pp. 553-558.

34. C.J. Henri, and T.M. Peters, "Three dimensional reconstruction of vascular trees. Theory and methodology," Med. Phys. **23**:197-204 (1996).

FIGURE LEGENDS

Figure 1. The same linear projections are produced by different 3D curves lying within an epipolar plane. The projections of the first point on each 3D curve are shown by dotted lines. Epipolar lines are shown on each viewplane.

Figure 2. Configuration of an epipolar volume. If reconstruction were to be performed from orthographic projection, the epipolar volume would resembe a box. Under perspective projection, this box becomes distorted. Associated epipolar regions are drawn in solid lines on each viewplane.

Figure 3. Incorrect solution provided by the simple use of epipolar lines to pair pixels. **A** shows 2 planar curves with dotted epipolar lines connecting paired points on both views. **B** shows the same curves, but the second curve is misplaced downward on the viewplane. Point 3 on the first view will fail to find an immediate match with the curve on view 2. If epipolar lines are used to find the first point on view 2 that can pair with point 3 on A's view, a severely incorrect distant match will be chosen. A better solution is provided by a regional solution that skips over points on curve 1, as shown in **C.**

Figure 4. Match values for a curve on view A (left) against several curves on view B (right). **A.** There is no intersection between the two curves. The match value is 0. **B.** There is a perfect match between the two curves; the program never performs a directed search. The match value is 150 (the number of 3D points created by the 2 curves). **C.** The same curve shown in **B** but an error of 2D curve definition makes the curve at right rise too high. The program will become lost

at the apex of the curves, perform a directed search, and find itself again. A penalty is exacted. The match value is 147. **D.** There is an imperfect match between the two curves; the match value here might be 70. **E.** The reconstruction program becomes lost at the apex of curve A. The 2D search length exceeds the program maximum and the pixel at the top of curve B is far away from curve A. The curves diverge from each other too much to make a likely match. The match value is 0. **F.** The curve on view A is associated on view B with 2 short curves, separated by another, thicker vessel's projection. The match value for the curve on view A with B1 is calculated as the sum of the points produced by A's sequential match with B1 and B2. No penalty is exacted for the interruption produced by another projection, although a 3D point may be lost because of the interruption. The match value of A with B1 is 149. The match value of the short curve B1 with A is the smaller value produced by reconstruction of A and B1 alone.

Figure 5. AP and lateral view of one of the datasets used for reconstruction. In these small (256x256 pixel) display windows, only the skeletons are shown. The projection of a single 3D curve of average length is shown in color. Some of the 3D curves reconstructed were much longer; some were so short as to occupy only 4 pixels on one or both projection views.

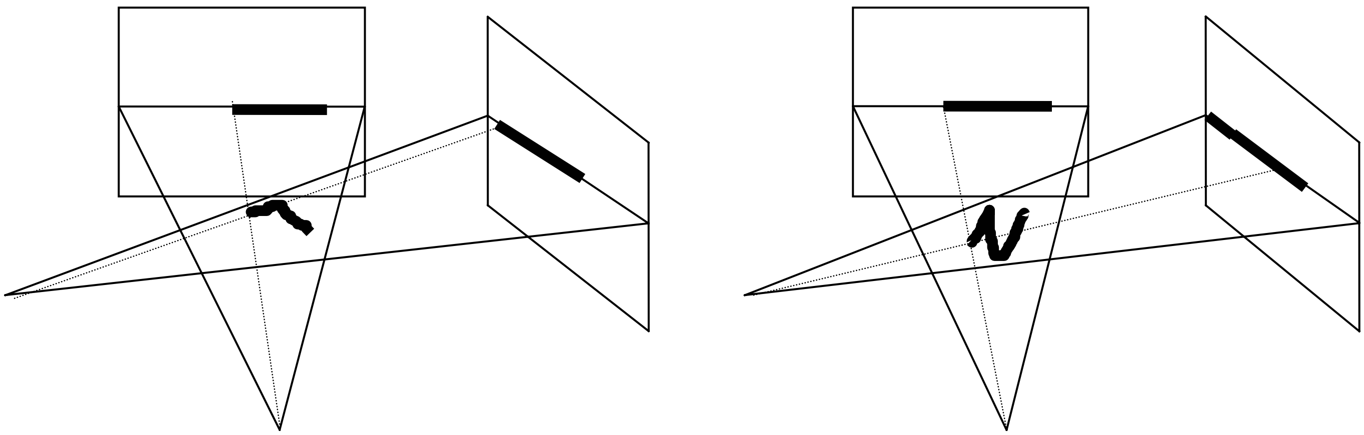

Fig 1. Bullitt et al (Algorithms) MPH

ORTHOGRAPHIC EPIPOLAR VOLUME PERSPECTIVE EPIPOLAR VOLUME

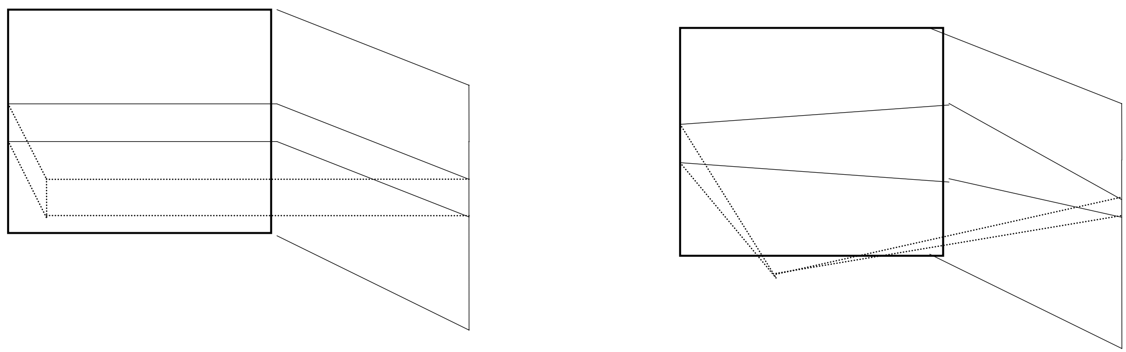

Fig 2. Bullitt et al (Algorithms) MPH

4’

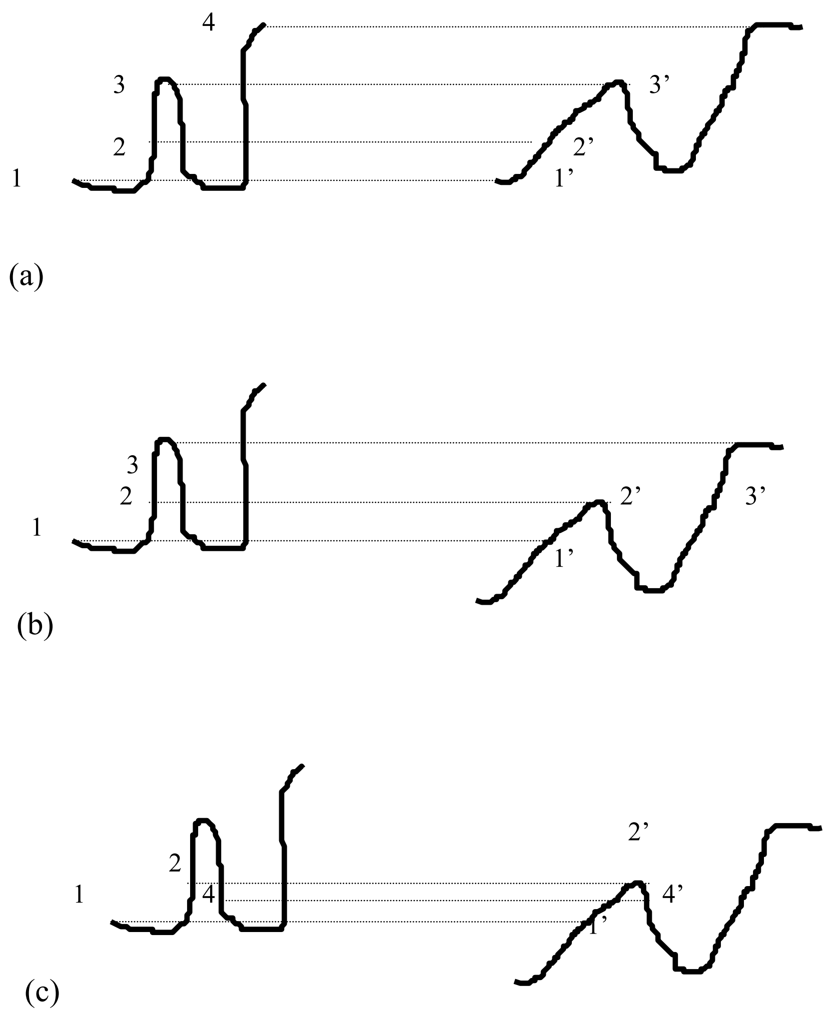

Fig 3. Bullitt et al (Algorithms) MPH

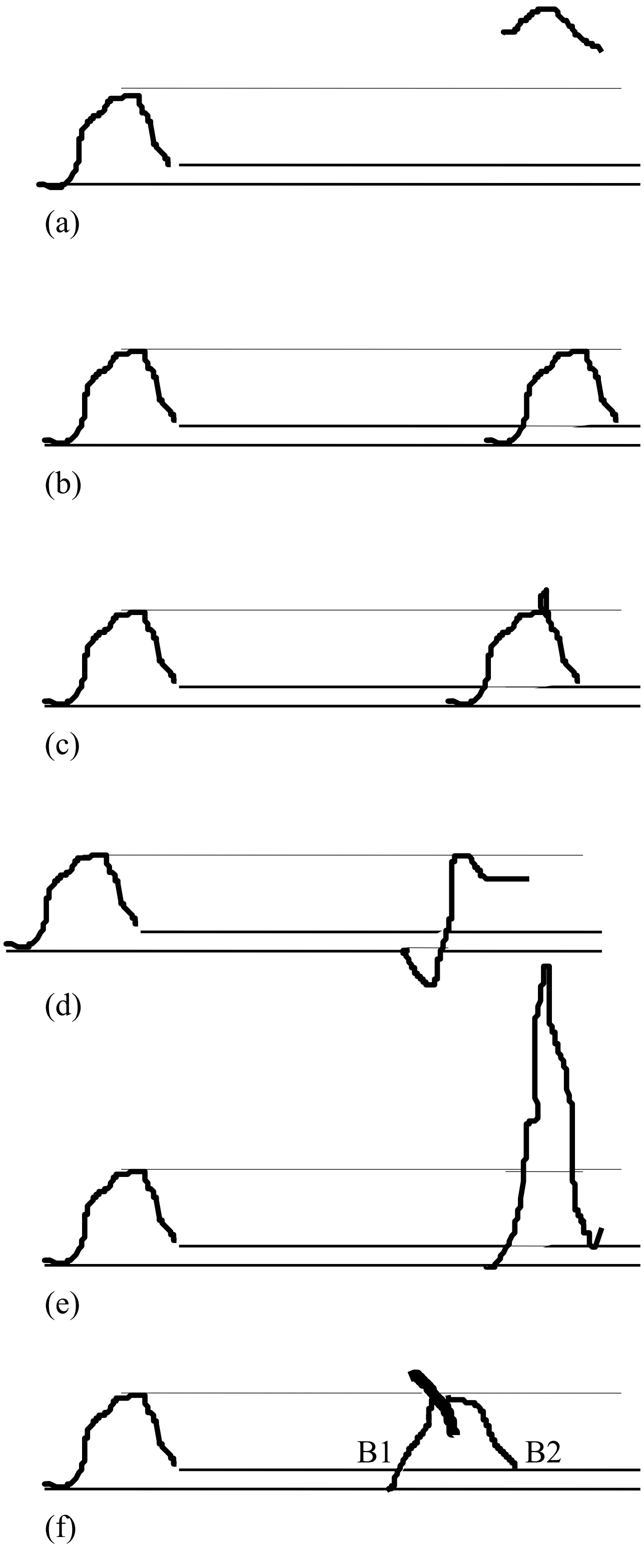

Fig 4. Bullitt et al (Algorithms) MPH

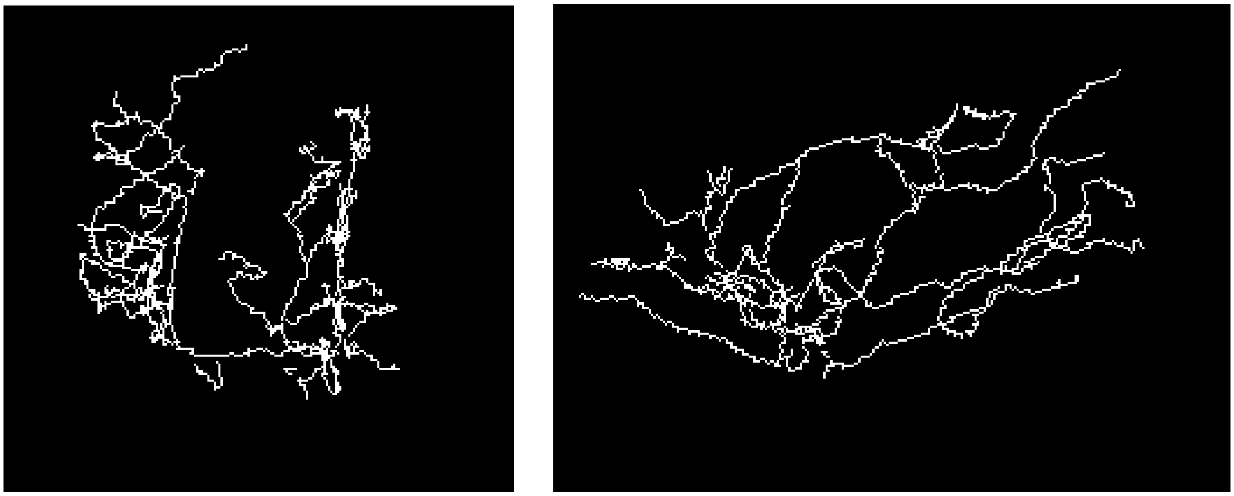

Fig 5. Bullitt et al (Algorithms) MPH